Proceedings of the 3rd IASME/WSEAS Int. Conf. on FLUID DYNAMICS & AERODYNAMICS, Corfu, Greece, August 20-22, 2005 (pp287-292)

Mechanism of Injectivity Loss During Water-Alternating-Gas (WAG) Injection

MEHRAN SOHRABI and MAHMOUD JAMIOLAHMADY
Institute of Petroleum Engineering,
Heriot-Watt University
Riccarton, Edinburgh, EH14 4AS
SCOTLAND, UNITED KINGDOM
Mehran.Sohrabi@pet.hw.ac.uk, Jami.Ahmady@pet.hw.ac.uk, http://www.pet.hw.ac.uk

Abstract: Many of current oil reservoirs are approaching the end of their waterflooding life. At this stage a significant quantity of oil (40-60%) will still remain in the reservoir. It is known that using the Water-Alternating-Gas (WAG) injection some of that oil can be produced. The WAG scheme is a combination of two traditional techniques of improved hydrocarbon recovery: waterflooding and gas injection.
In many reservoirs, injectivity during WAG cycles has been lower than expected. In many cases the low injectivity rates prolong injection time and play havoc with project economics. Therefore, injectivity loss is a crucial limiting factor in many projects involving WAG injection. In an example, the pre-WAG water injection rate of 286 m^3/d (1800 BPD) was not pressure-limited, while after a couple of WAG cycles the gas and water injection rates were limited by pressure to about 160 and 130 m^3/d (1000 and 800 BPD), respectively. Currently, there are no clear explanations of the factors influencing injectivity loss during WAG injection, nor methods available to mitigate this problem.
In this paper we report results of an experimental study that was carried out to directly visualize the pore-scale events taking place during WAG injection in porous media. We show that, in the absence of other relevant causes, gas trapping causes relative permeability reduction and injectivity loss.

Key-words: - WAG injection, Injectivity loss, Micromodel, Relative permeability, Water flood

1 Introduction

The Water-Alternating-Gas (WAG) scheme is a combination of two traditional techniques of improved hydrocarbon recovery: waterflooding and gas injection [1]. Conventional gas or waterfloods of an oil reservoir usually leave at least 50% of the oil as residual. WAG injection is a proven method for recovering some of that residual oil. The first field application of WAG is attributed to the North Pembina field in Alberta, Canada, by Mobil in 1957. Since then WAG injection has been successfully performed in many oil reservoirs worldwide. However, there have been a number of practical problems including reduction of the rate of water injection (injectivity loss) after injecting gas.

Injectivity has a direct impact on project economics, and loss of infectivity in WAG projects is an area of concern. Experience to date has been that most projects will experience some loss of infectivity during the water injection cycle of the WAG process, with the average being about 20%. However, there have been cases reported where the loss of water infectivity has been severe [2].

Injectivity loss appears to be common during the water halfcycle for both low and medium permeability reservoirs and during the gas cycle for low permeability reservoirs. With low viscosity and high mobility, one would expect increased gas injection rates. A number of field solutions for improving injectivity have been attempted with mixed results. Currently, there are no clear explanations of the factors influencing WAG injectivity loss, nor methods available to mitigate this problem.

The aim of this study was to perform WAG experiments in high-pressure glass micromodels to investigate the physics of the WAG process and investigate mechanisms of injectivity loss and possible prevention or remediation strategies.

2 Experimental Set-up

2.1 The High Pressure Micromodel Rig

A high pressure micromodel rig was used to perform the WAG experiments at pressures of up to 6000 psia and at a temperature of 100 °F. It is shown schematically in **Fig**. **1**. The rig consists of the following major parts:

High Pressure Fluid Storage Vessels. Three high-pressure stainless steel vessels are used to store the injection fluids and one to collect produced fluids from the micromodel. All the vessels are pressure rated to 6000 psia.

Constant Temperature Fluid Storage Chamber. This
chamber is used as a constant temperature oil bath to maintain the fluids in the fluid storage vessels, and all the necessary fluid path lines and fittings, at the constant test temperature of 100 °F.

Constant Temperature Micromodel Housing Chamber. This is similar to that of the fluid storage chamber and is used to maintain the micromodel at constant temperature equal to the temperature of the test fluids.

Low Rate Pumps. Two accurate low rate pumps are used to control fluid flow through the micromodel. The rates of injection and production range from a low of 0.01 cm3/h to a maximum of 100 cm3/h. With the micromodel that was used in the set of experiments reported here, 0.01cm3/h is equivalent to an estimated velocity of about 1.2 m/d for single-phase flow

Computer Controlled Linear Drive System. A computer controlled linear drive system is used in the tests, which allows a magnifying camera to be positioned automatically at any part of the micromodel, and sequentially or continuously sweep the micromodel for video recording. The camera is capable of working at a magnification of up to 400 times. **Fig. 2** shows the optical system of the rig.

Glass Micromodels. A two-dimensional pore structure is etched onto the surface of a glass plate, which is otherwise completely flat. A second glass plate is then placed over the first, covering the etched pattern and thus creating an enclosed pore space. This second plate, the cover plate, has an inlet hole and an outlet hole drilled at either end, allowing fluids to be displaced through the network of pores (**Fig. 3**). Because the structure is only one pore deep, and the containing solid walls are all glass, it is possible to observe the fluids as they flow along the pore channels and interact with each other. It is also possible to observe how the geometry of the pore network affects the patterns of flow and trapping.

2.2 Test Fluid

The equilibrated fluids used in the experiments consisted of distilled water, n-decane and methane. To distinguish between the liquid hydrocarbon and the aqueous phase, the colour of the n-decane was changed to red using a hydrocarbon soluble dye (Sudan Red), and similarly, the colour of the water was changed to blue using a water soluble dye (Methyl Blue). Both the blue water and the red n-decane were filtered using fine filter papers to remove any undesolved dye particles.

Fluid Preparation. Filtered blue water and methane were brought into equilibrium at the desired pressure and temperature. The same procedure was followed for the equilibration of gas and oil. The solubility of oil in water was considered to be negligible (at 500 psia and 100 oF).

Fluid Properties. The equilibrium properties of the water, ndecane, methane system at 500 psia and 100 °F and the effect of dye, where shown, are estimated as follows:

	Density/ g.cm-3
Water (**H2O**+C1+dye) [3,4]	1.0026
Oil (**nC10**+C1+dye) [5]	0.7062
Gas (**C1**+nC10) [5]	0.0209
	Viscosity/ mPa.s
Water (**H2O** +C1+ dye) [3]	0.658
Oil (**nC10**+C1+dye) [5-7]	0.597
Gas (**C1**+nC10) [5-7]	0.010
	Interfacial Tension/mNm-1
Gas/Oil [6]	15
Gas/Water [8]	65
Oil/Water [8]	41

So/w.g = Spreading Coefficient of oil over water = + 9 mNm-1.

The effect of dye on density and viscosity of the liquids at micromodel conditions of 100 oF and 500 psia has been calculated. The positive value of the spreading coefficient indicates that there will always be a visible layer or a film of oil spread between gas and water. The resolution of the images does not permit the viewing of the thin oil films, which can be on the order of one nanometer across.

3 Test Procedure

Initially, the micromodel was saturated with clear distilled water and pressurised to 500 psia and subsequently displaced with blue live water, equilibrated with gas at 500 psia and 100 ^{o}F. To simulate the primary drainage (initial migration of oil into the water bearing porous medium), equilibrated oil (red n-decane), was injected from the top of the vertical micromodel, and continued until oil reached the base of the micromodel. To avoid oil getting into the lower pipes containing the water and gas phases, the oil flood was stopped at the bottom of the micromodel. **Fig**. **4** shows an example of a section of the micromodel when 100% saturated with equilibrated blue water, with

Fig. 5 showing the connate water saturation, established after oil injection. In both cases the micromodel was scanned vertically in 10 separate sections. In these Figures, and throughout this report, only the image of the middle section is presented.

The model was then waterflooded at a low rate of 0.01 cm^3/h from the base to establish the waterflood residual oil saturation (S_{orw}). This rate corresponds to a capillary number of 2.52E-7, using single-phase flow area, and 5.04E-7 for two-phase flow area. The magnitude of capillary number indicates a capillary dominated flow regime, which is consistent with the observations. Water was observed to flow mostly through the sharp corners of the pores (as can be visualised in the corners of a square tube). The water layers surrounding the oil were seen to thicken progressively leaving oil filaments in the middle of pore bodies and finally causing oil snap off at some pore throats. The fluid distribution in the micromodel at the end of water flooding is shown in **Fig. 6**.

Fig. 7 is a magnified image of a section of the micromodel at the end of primary drainage of water (oil injection through water saturated micromodel), which demonstrates the relative position of the wetting phase (blue water) and non-wetting phase (red oil), in a strongly water-wet micromodel. The small pores and the dead-end pores are mostly occupied by water. The direction and the shape of the water-oil interfaces are good indication of strongly water-wet conditions. Also some relatively large pores in **Fig. 8** are filled with water, as these pores are surrounded by smaller pore throats from which water could not be displaced by the oil, because its pressure did not exceed the oil-water capillary pressure. **Fig. 8** shows a magnified image of the same section of the micromodel at the end of the waterflood.

Comparison of **Figs 7** and **8** highlights that during waterflooding oil was displaced by corner and layer flow of water rather than by a piston-like displacement. The slow thickening of water filaments at the sides and corners of oil filled pores during water flooding was a consequence of a capillary dominated flow regime.

After this initial waterfllooding, WAG injection commenced. Each WAG cycle began with gas injection and ended with water injection. Five cycles of WAG injection were conducted. In each cycle, the injection of gas or water continued until no further oil production or change in fluid distribution occurred. To distinguish the colourless gas from the colourless glass (resembling grains in a natural porous medium), gas was digitally coloured in yellow, using an image analysis computer program. **Fig. 9** shows the fluid distribution in the micromodel after the first cycle of gas injection, with the blue, red and yellow colours representing water, oil and gas respectively. As it can be noticed, the gas has made a continuous path to flow through the micromodel. At the end of this gas injection, water injection commenced again at the same rate of 0.01 cm^3/h (~ 1.2 m/d). During water injection, corner flow of water resulted in water layers surrounding the gas occupied pores to thicken until the gas blobs became unstable and finally collapsed. The snap-off of the gas phase occurs as a result of capillary competition between the different phases. **Fig. 10** shows the fluid distribution in the micromodel after the water injection period of the first cycle. The fragmentation of the gas blobs is clearly observed. As a result of this gas fragmentation, the gas blobs become trapped in the porous medium (micromodel).

Alternating gas and water injection continued until five cycles were completed. **Figs. 11** and **12**, and **Figs. 13** and **14,** show the results of the second and the fifth WAG cycles respectively. In each WAG cycle a sequence of events similar to what was explained for the first one occurred. Comparison of **Fig. 14** with **Fig. 9** shows that more gas has been trapped as the WAG cycles were repeated and also more oil has been recovered.

4 Discussion

During the initial waterflood, as water was the wetting phase and the rate of water injection was well within capillary dominated regime, water flowed in the corners of the pores in the form of layers surrounding the oil present in the larger pore bodies. These water layers were seen to thicken progressively leaving oil filaments in the middle of pores and finally causing oil snap off at some pore throats. This oil is what is referred to as residual oil to waterflood. To see how much of this residual oil could be recovered by WAG injection and how the injectivity is affected, five WAG cycles were carried out.

During the first gas injection period, as the IFT between gas and oil is less than the IFT between gas and water, when faced with pores of equal radius, gas prefers to enter those filled with oil. The invasion of oil filled pores by gas causes a small bank of oil to move ahead of gas front. The oil flowing ahead of the gas is added to the oil already present in those pores, resulting in an improvement in the oil mobility. During the subsequent water injection, water invades the gas

filled pores. Consequently, the gas channels become narrower as the water layers grow, and finally the gas becomes fragmented due to snap off which takes place at some pore throats. This causes the trapping of the broken gas blobs in the pores which in turn causes relative permeability reduction and hence loss of fluid injectivity.
As more WAG cycles (gas and water slugs) are injected, more gas becomes traps and hence the flow of fluids is more restraint.

5 Conclusions

The results of the reported experiment, which was performed in strongly water-wet glass micromodel, show that relative permeabilities and saturation changes reduce injectivity when the system switches from one injection fluid to another.
Water slugs injected subsequent to gas slugs cause fragmentation and trapping of the gas in the pore space which reduces the area available to water flow and hence relative permeability reduction. The amount of gas trapping, amongst other things, is a function of IFT between oil and gas. This suggest that further tests is necessary to investigate the IFT as a way to characterize the optimum gas/oil IFT to minimize gas trapping and hence injectivity loss.

6 References

[1] Surguchev, L.M. *et al.:* "Screening of WAG Injection Strategies for Heterogeneous Reservoirs," paper SPE 25075 presented at the 1992 SPE European Petroleum Conference, Cannes, France, 16–18 November.

[2] Hnrvey, M. T., Shelton, J. L., ad Kelm, C. H.: "Field Injcctivity Experiences with Miscible Recovery Projmts Using Alternate Rich-Gas and Water Injection: JPT September 1977 p1051-l055.

[3] Amyx, J. W., Bass, D. M. and Whiting, R. L., "Petroleum Reservoir Engineering", McGraw-Hill Book Co., Inc., 1960, pp 457-59.

[4] Danesh, A. "PVT and Phase Behaviour of Petroleum Reservoir Fluids", ELSEVIER, 1998.

[5] Reamer, H. H., Olds, R. H., Sage, B. H. and Lacey, W. N. "Phase Equilibria in Hydrocarbon Systems – Methane-Decane System", Industrial and Engineering Chemistry, Vol.34, No. 12 Dec 1942, pp1526-31.

[6] Stegemeier, G. L., Pennington, B. F., Brauer, E. B. and Hough, E. W., "Interfacial Tension of the Methane-Normal Decane System", SPEJ, Sept. 1962, pp. 257-260.

[7] Lohrenz, J., Bray, B. G. and Clark, C. R., " Calculating Viscosities of Reservoir Fluids from Their Compositions", JPT, October 1964, pp 1171-76.

[8] Firoozabadi, A. and Ramey, Jr., H. J., "Surface tension of water-hydrocarbon systems at reservoir conditions", The Journal of Canadian Petroleum Technology, May-June 1988, Vol.27, No.3.

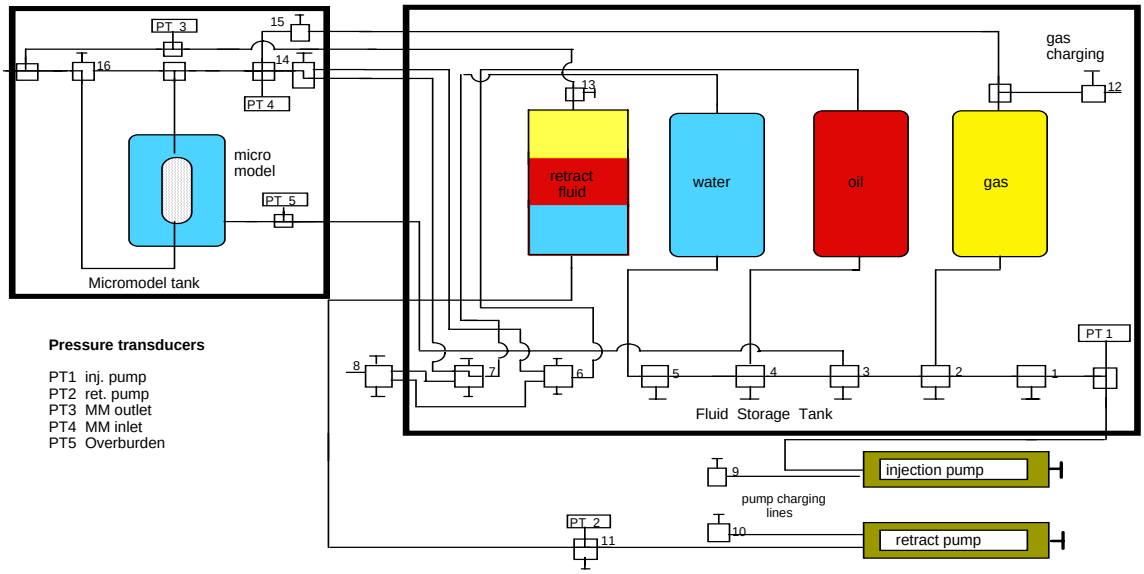

Fig. 1-Schematic diagram of the high-pressure micromodel rig

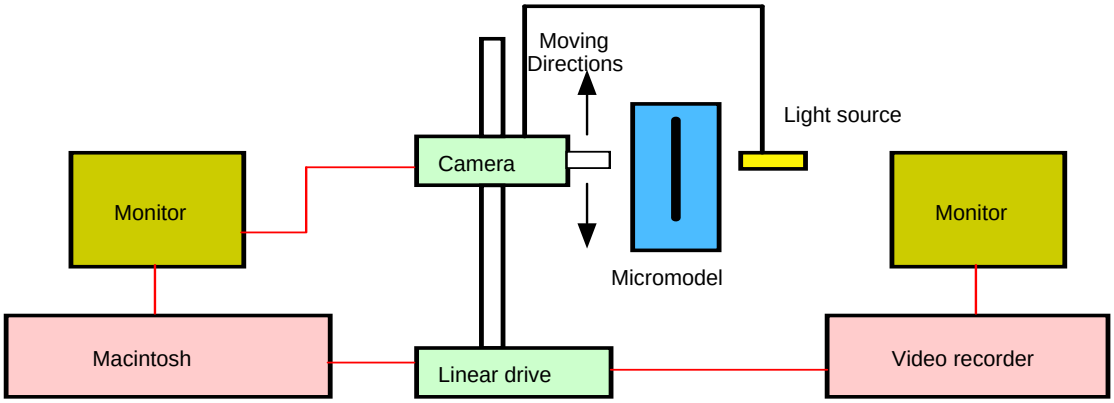

Fig. 2-Schematic diagram of Optical System

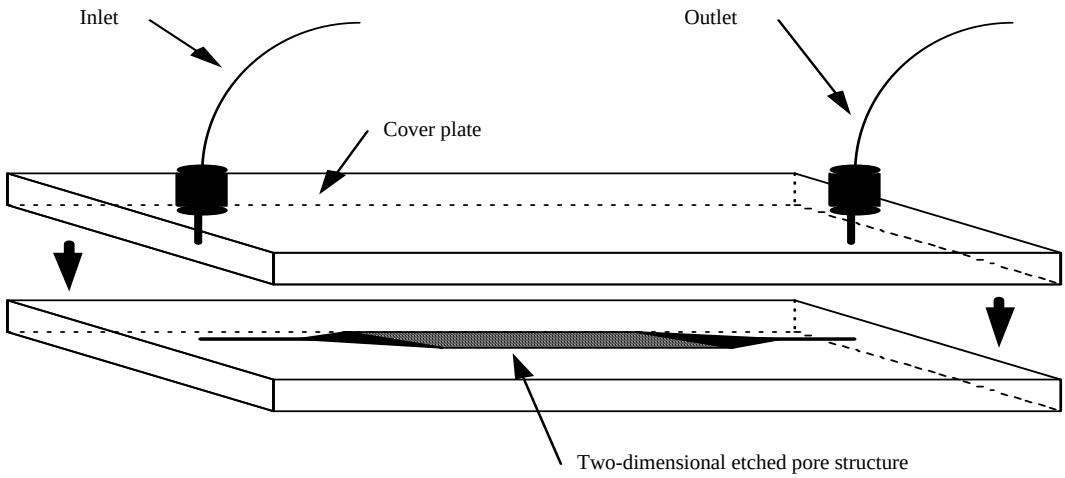

Fig. 3: The etched plate and the cover plate are brought together to form an enclosed pore space through which fluids can be displaced.

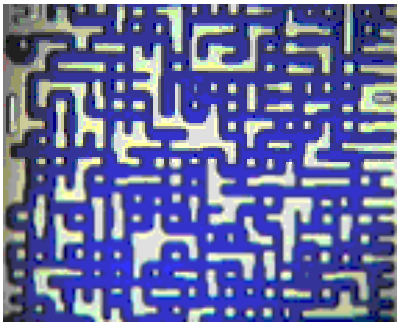

Fig. 4-100% water saturation

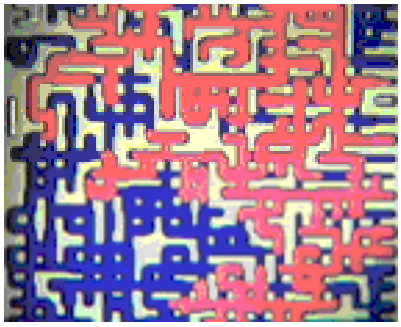

Fig. 5-Primary drainage of water

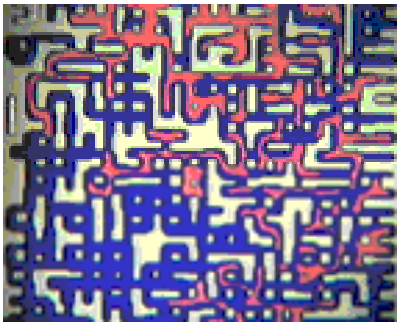

Fig. 6-Initial waterflood

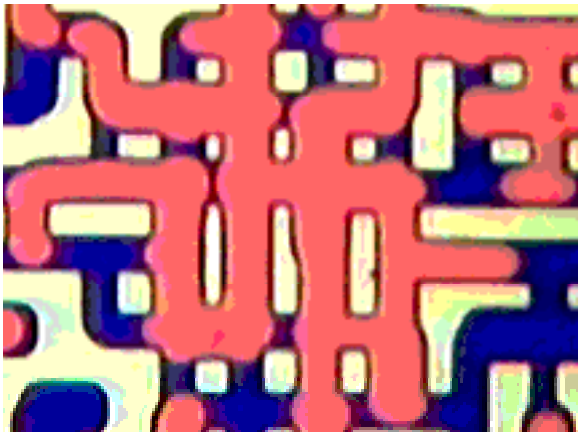

Fig. 7-Water/oil distribution before waterflood

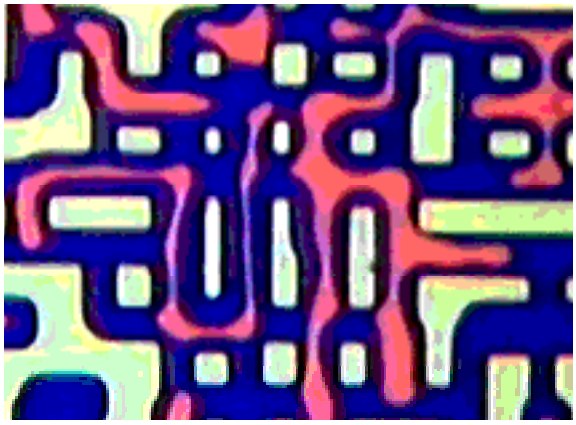

Fig. 8-Water/oil distribution after waterflood

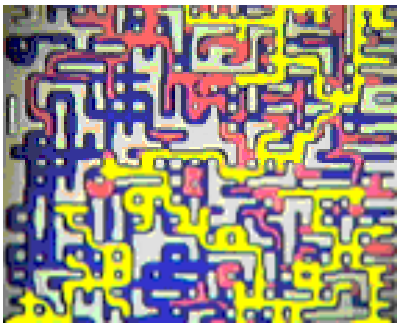

Fig. 9-First cycle gas injection

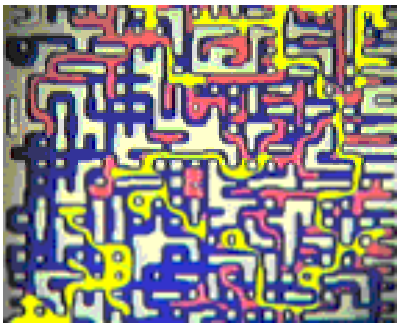

Fig. 10-First cycle water injection

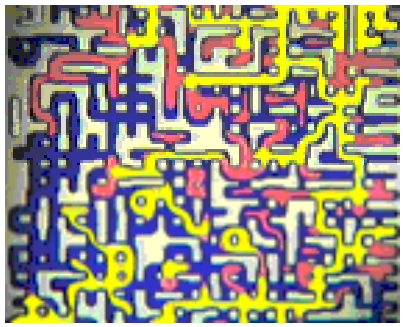

Fig. 11-Second cycle gas injection

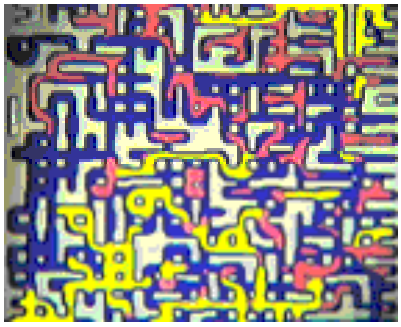

Fig. 12- 2nd cycle water injection

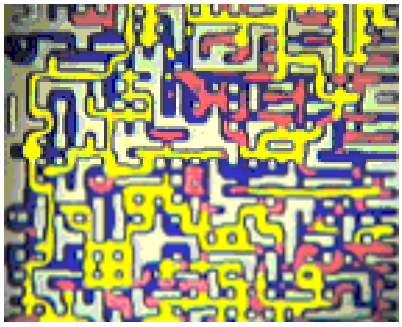

Fig. 13-Fifth cycle gas injection

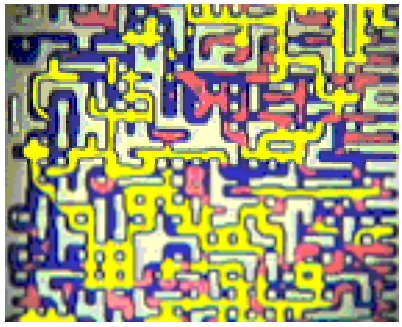

Fig. 14-Fifth cycle water injection